Characteristics of a Gaussian focus embedded within spiral patterns in common-path interferometry with phase-apertures

Yizhou Tan[a,b] , Ying Gu[a,b*]
[a] Department of Laser Medicine, the First Medical Center, Chinese PLA General Hospital, 28 Fuxing Road, Beijing, China,100853
[b] Laser Medicine Center, Hainan Hospital, Chinese PLA General Hospital, Haitang Bay, Sanya, China, 572013

Supplemental Materials: Phase only transform by double-ring phase-aperture

The quantitative analysis of coherent combination between the vortex beam and concentric Gaussian beam was performed according to the following theoretical model.
The double-ring phase-aperture is made of a transparent element divided into two parts: the inner circle zone of radius r_1 and the ring zone between r_1 and the outer radius r_2.
The light beam conversion process is shown in Fig.S1 (a). The Gaussian laser illuminates vertically on the double-ring phase-aperture, the diffracted field amplitude distributions for the phase-aperture is expressed by Eq.(S1) [20 21 38]. The vortex field illuminates vertically on a circle aperture, the diffracted electric field distributions $E(x, y)$ for the circular aperture is expressed by Eq. (S2) and Eq.(S3).

Diffraction of Gaussian beam: Let us consider an incident beam illuminate the phase-aperture, the amplitude $A(\sigma, r)$ of the output light is determined by the radially symmetrical Fourier transform as follows:

$$A(\sigma, r) = \int_0^{r1} A_0(r) \cdot J_0\left(k\sigma r/f\right) \cdot r dr \qquad \text{(Inner circle zone)}$$

$$A'(\sigma, r) = \int_{r1}^{r2} A'_0(r) \cdot J_0\left(k\sigma r/f\right) \cdot r dr \qquad \text{(Ring zone)}, \qquad \text{(S1)}$$

where the incident Gaussian laser wavenumber $k = 2\pi/\lambda$, wavelength λ; $A_0(r)$ and $A'_0(r)$ are the amplitude of electric field $E(r)$ in the input plane. $J_0(k\sigma r)$ is the Bessel function of the zero order, σ is geometric factor, f is the focal length of the lens. In x-y coordinate system,

$r = \sqrt{x^2 + y^2}$ [21]. r_1 and r_2 represent the radius of the double-ring phase-aperture[20 21].

Diffraction of orbital angular momentum carrying optical beams:
The vortex light is propagating in the + z direction, the electric field $E(x', y')$ is expressed as

$$E(x', y') = \exp\left(-\frac{x'^2+y'^2}{\omega_0^2}\right) \cdot \left(-\frac{x'^2+y'^2}{\omega_0^2}\right)^{\frac{l}{2}} \cdot \exp\left[jl \cdot tan^{-1}\left(y'^2/x'^2\right)\right], \qquad \text{(S2)}$$

where l is the topological charge ($l \neq 0$), and ω_0 is the waist width of the vortex beam. Coordinate (x, y, z) denotes the light propagation space.

Consider the vortex field incident normally on a circle aperture occupying the z = 0 plane. Here the circle aperture is formed by the inner circle zone, which has a complex transmittance function $\boldsymbol{T}$ (x ′, y ′). The observation plane at a distance z = *d* from the aperture. Under paraxial approximation the diffraction integral formula for the electrical field distribution at the point *P* is

$$E_P(x,y) = \frac{1}{j\lambda}\int_{x1}^{x2}\int_{y1}^{y2} E\left(x',y'\right)\cdot T\left(x',y'\right)\frac{\exp(jkr)}{r}dx'\,dy' \quad \text{(Circle aperture)}, \quad \text{(S3)}$$

where *k* is the wave vector, *r* is the distance from the point *P* to any point $\left(x',y'\right)$ at the diffraction plane. In (x, y, z) coordinate, $r = \sqrt{x^2+y^2+z^2}$ [25 39 40].

The diffracted electric field distributions $E(r,\theta)$ of the annular aperture is proportional to the *l*-order Bessel function $\boldsymbol{J}_l$:

$$E(r,\theta) \approx J_l(\alpha r)\cdot\exp(il\theta), \quad \text{and} \quad \alpha = 2\pi R\,/\,\lambda d \quad \text{(Annular aperture)}, \qquad \text{(S4)}$$

where (r,θ) are the usual polar coordinates and 2*R* is the diameter of the diffracting disk. *d* is the distance between the obstacle and the observation zone [4 24].

Note: the vortex field illuminates on a polygon-aperture, the diffracted electric field distributions $E_P(x,y)$ are calculated by the Eq.A (3) with the integral boundary conditions for corresponding polygon- geometry area [5 6].
The diffracted electric field distributions $E(r,\theta)$ of the annular aperture is expressed by Eq.(A4). For *l* = 0 we obtain the diffracted electric field distribution for the fundamental Gaussian beam by Eq. (A3) and (A4). In far field the diffracted intensity distribution $I_p(x,y) = \left|E_p(x,y)\right|^2$.

Interference between two diffraction fields:
Case I: Let us consider separately the inner circle zone which outputs a vortex beam in Fig. A1(b), and its circular phase-aperture generates the diffraction electric distribution $E_{circular}(x,y)$ in far field that has the diffracted intensity distribution with doughnut-like shape, as shown in Fig.A1(c). Then consider separately the ring zone which outputs a Gaussian beam in Fig. A1(d), and its annular phase-aperture generates the diffraction electric field $E_{annular}(x,y)$ in far field that creates the *Poisson* diffraction spot on the optic axis in Fig.A1(e) [4 24]. The cross-section intensity distribution of $E_{circular}(x,y)$ and $E_{annular}(x,y)$ is plotted in Fig.A1(f).

Interfering the optical vortex beam $E_{circular}(x,y)$ with a Gaussian diffracted wave $E_{annular}(x,y)$ will transform the azimuthal phase variation of the pattern into an azimuthal intensity variation. The constructive interference occurs at the position where the phase difference of the two diffracted beams is zero and the peak is generated. At the same time, the decreasing occurs at the position of two diffracted beams with opposite phase. When the coherent superposition between $E_{circular}(x,y)$ and $E_{annular}(x,y)$ occurs in far field, the

resulted compound pattern is in the shape of spiral petal-like fringes with the brighter Poisson spot in the middle in Fig.3(b, c).

Case II: In Fig.A1(h), the circular phase-aperture outputs a Gaussian beam, which generates the diffraction fringes $E_{circular}(x, y)$ in far field, called as *Airy* spot for a circular aperture in Fig.A1(i). In Fig.A1(j), the ring zone output a vortex beam, and its annular phase-aperture generates the diffraction field $E_{annular}(x, y)$ with doughnut shape, as shown in Fig. S1(k). The coherent superposition between $E_{circular}(x, y)$ and $E_{annular}(x, y)$ resulted in a compound pattern in far field, which is in the shape of propeller-like fringes with the brighter *Airy* spot in the middle, shown in Fig. S1(l) and Fig.3(e, f).

In section §2, we analyze the theory and method for shaping the light optical wavefront by employing a transmissive spatial light modulator (SLM). The transmission-mode SLM is a necessary condition for realization common-path interference (Fig.1 and Fig.S1).

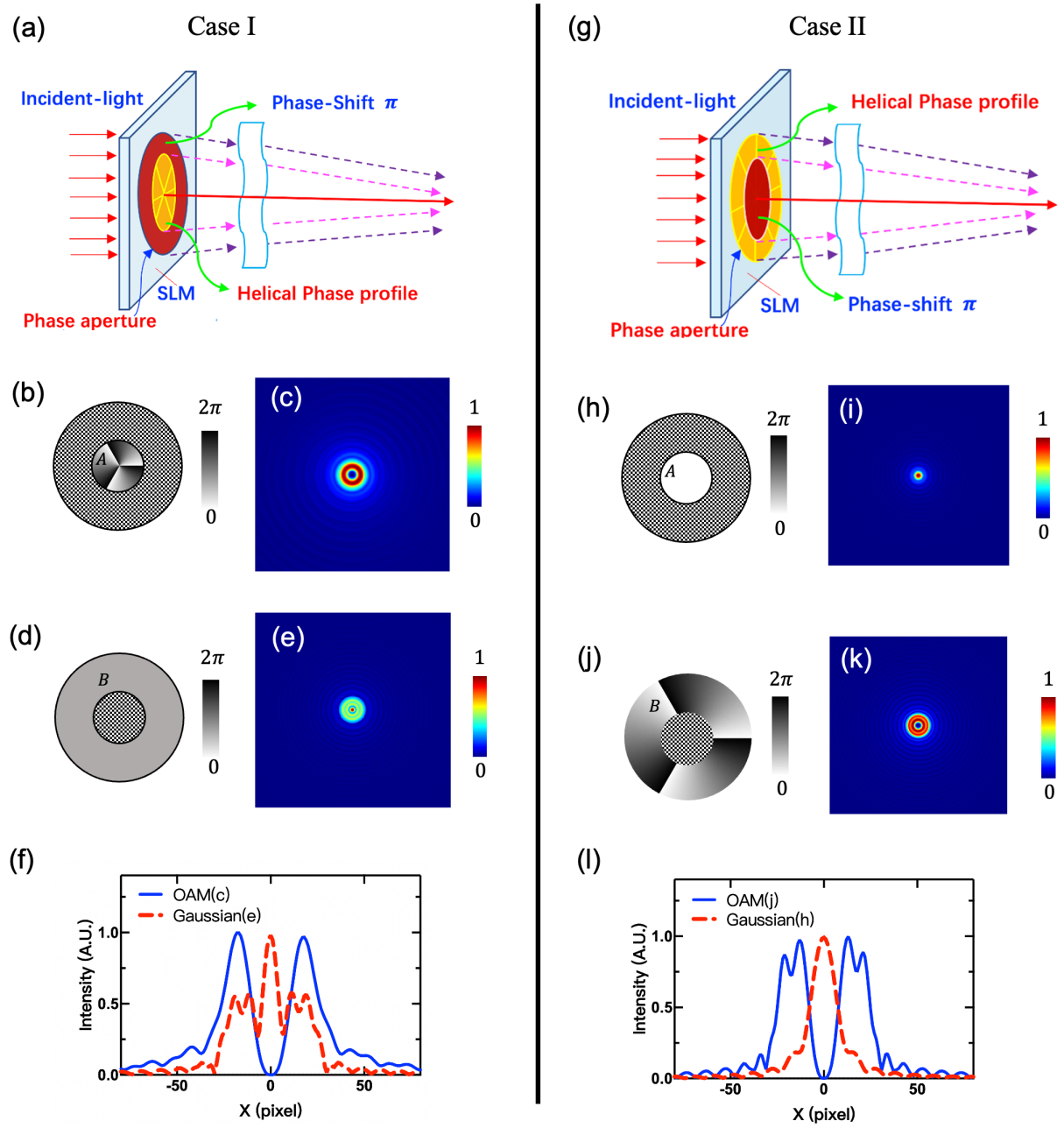

Fig. S1 Interference between diffracted vortex beam and diffracted plane wave beam.

(a) Case I: the structural diagram of double-ring phase-aperture element in common-path interferometer.

(b) Light beam illuminates the circular phase-aperture with helical phase modulation profile. (c) Diffracted intensity distribution of the vortex beam from (b). (d) Light beam illuminates on the annular part of the phase-aperture. (e) Diffracted intensity distribution of Gaussian laser from annular phase-aperture (d). (f) Normalized cross-section intensity of (c) and (e).

(g) Case II: the structural diagram of double-ring phase-aperture element in common-path interferometer. (h) Light illuminates on the circular phase-aperture. (i) Diffracted intensity distribution of Gaussian laser from (h). (j) Light

illuminates on the annular part with helical phase modulation profile. (k) Diffracted intensity distribution of vortex beam from annular phase-aperture (j). (l) Normalized cross-section intensity of (i) and (k).

* The shaded area on double-ring phase-aperture is assumed without light passing through.

Effect of phase-aperture size on the diffraction-interreference pattern

We study the effect of the size of the phase-aperture on the diffraction-interreference pattern. The diameter d of the circular phase-aperture and side length d of the rectangular phase-aperture are set to 100, 300, 600, 900 pixels individually (the SLM width is 1080 pixels in our experiment). By adjusting d, we observed the revolving of the diffraction-interference patterns from a Gaussian spot to a doughnut-shape intensity pattern of an optical vortex, results shown in Fig.A2.

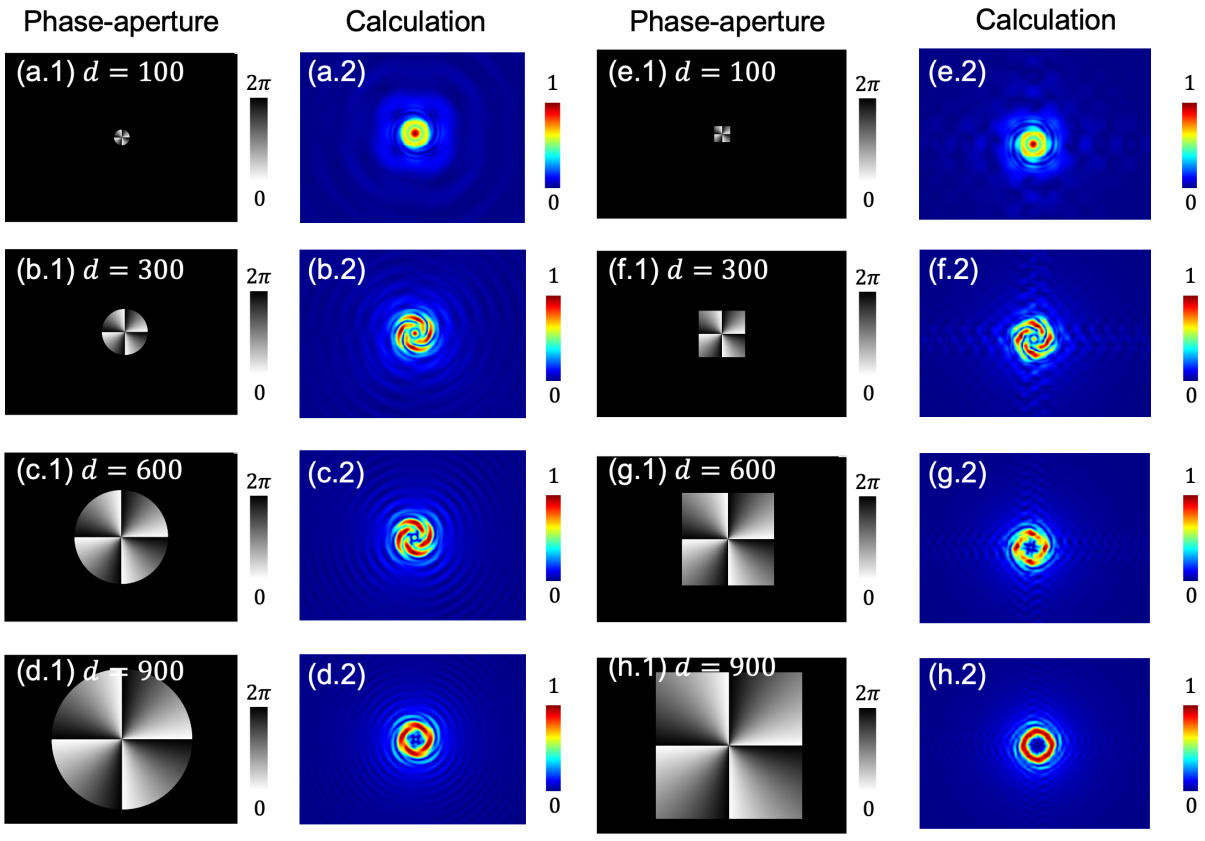

Fig.S2 The effect of size of circular and rectangular phase-aperture on the diffraction-interreference pattern

(a.1-d.1) A circular phase-aperture with helical phase ($l = 4$) modulated profile in the inner circular zone. And the circular has the diameter d, the outer ring of radius r_2. (a.2-d.2) Numerically simulated intensity distribution. (e.1-h.1) A rectangular phase-aperture with helical phase ($l = 4$) modulated profile in the inner circular zone. And the inner rectangle has the side length d, the outer ring of radius r_2. (e.2-h.2) Numerically simulated intensity distribution.